

Extraordinary spin in a generic electromagnetic field

Peng Shi*, Aiping Yang, Xiaojin Yin, Luping Du*, Xinrui Lei, Xiaocong Yuan*

Nanophotonics Research Centre, Shenzhen Key Laboratory of Micro-Scale Optical Information Technology, Institute of Micro/Nano Optoelectronics, Shenzhen University, 518060, China

* Authors to whom correspondence should be addressed: shipeng@szu.edu.cn, lpdu@szu.edu.cn, and xcyuan@szu.edu.cn

Abstract: Electromagnetic spins, including longitudinal and transverse ones, have been playing important roles in light-matter interactions, leading to many intriguing phenomena and applications. Previously, the ordinary longitudinal and transverse spins of single polarized modes were distinguished by means of mean wavevector. However, our recent discovery argues that this method is incomplete for a generic electromagnetic field with hybrid polarization. Here, we demonstrate, both theoretically and experimentally, an extraordinary transverse spin oriented parallel to the mean wavevector and an extraordinary longitudinal spin perpendicular to the mean wavevector. Remarkably, the extraordinary transverse spin is locally helicity-dependent, resulting in a corresponding helicity-dependent spin-momentum locking, while the helical property of integral transverse spin is determined by the symmetry breaking of system. Furthermore, this extraordinary transverse spin determines the inverted helical component and thus is related to the geometric phase closely. The findings have deepened the understanding the underlying physics of spins and opened an avenue for chiral quantum optical applications.

Main Text: Spin angular momentum (SAM) is a fundamental dynamical property of elementary particles and classical wave fields [1-5]. For a classical electromagnetic (EM) field, SAM in associated with the circular polarizations of electric and magnetic fields can be oriented in an arbitrary direction. It is well-known that the SAM component oriented along its propagating direction and helicity-dependent is considered as the longitudinal spin (L-spin) [6], whereas the transverse spin (T-spin) representing the helix-free SAM components orients perpendicular to the wavevector [7,8]. Till now, the T-spin has been investigated in various fields, including evanescent modes [8], guided wave modes [7], interference fields [9], Gaussian focused fields [7], unpolarized fields [10] and photonic chiral spin textures [11, 12]. EM spins can interact intensely with orbital angular momentum (AM) [13], especially in the subwavelength scale, leading to the appearance of research interests in spin-orbit interaction [6,14] and many fantastic phenomena [15-17], offering potential applications in the fields of optical manipulation [18], imaging [19] communications [20], metrology [21] and on-chip quantum technologies [22].

However, if the complicated structured properties [23], including the structures of intensity, phase and polarization, are introduced into the EM field, it is hardly to distinguish between longitudinal and transverse spins with wavevector directly. Previously, several researchers proposed to quantify the transverse properties of EM spins by complicated expressions [8] or mean wavevector $\bar{\mathbf{k}}$ [24]. These were illogical since a class of physical quantity should possess a unified physical mechanism, yielding a universal equation.

In quantum physics, spin is an intrinsic property for elementary particles. In the work, we extract the L-spin

following this idea. Remarkably, the remaining T-spin by subtracting the L-spin from the total spin can be expressed with a unified equation which reveals the T-spin is stemmed from the inhomogeneities of an EM field. Furthermore, we discover an extraordinary T-spin/L-spin is oriented parallel/perpendicular to the mean wavevector. Therein, the extraordinary T-spin is helicity-dependent, which results in the accompanied spin-momentum locking property of this T-spin as helicity-dependent concurrently. Additionally, this extraordinary T-spin determines the inverted helical component in the EM system and thus it is related to the geometric phase closely. We further evaluate the helicity-dependent properties of T-spins and spin-momentum locking experimentally, by mapping the three components of SAM in a focused beam with circular polarizations in our in-house developed near field imaging system. Our findings could be important for understanding the properties of EM spin with potential applications including optical manipulation, nanometrology and chiral quantum optics.

Generally, in an isolated system, photons tend to arrange parallelly to minimize the energy cost [25]. However, a plane wave is an idealized physical model and the real EM wave must be inhomogeneous, stemming from the intrinsic or extrinsic interactions, which leads to the structured SAM. Based on this consideration, we propose and prove theoretically that the L-spin (\mathbf{S}_l) and T-spin (\mathbf{S}_t) of an arbitrary time-harmonic monochromatic EM wave which can be expanded into the superposition of plane wave basis [2] can be expressed as (see [Supplemental Notes 1-4 for the proofs](#))

$$\mathbf{S}_l = \hbar\sigma \wedge \hat{\mathbf{k}}, \quad (1)$$

and

$$\mathbf{S}_t = \mathbf{S} - \mathbf{S}_l = \mathbf{S} - \hbar\sigma \wedge \hat{\mathbf{k}} = \frac{1}{2k^2} \nabla \times \mathbf{\Pi}, \quad (2)$$

where the EM helicity σ is expressed as the ratio of polarization ellipticity to the energy density [9]; $\mathbf{\Pi}$ the kinetic-Abraham-Poynting momentum [26] and \mathbf{S} is the total SAM; ω the angular frequency and \hbar the reduced Plank constant. Particularly, the canonical momentum $\mathbf{P} = \langle \psi | \hat{\mathbf{P}} | \psi \rangle / \hbar\omega$ with $\hat{\mathbf{P}} = -i\hbar\nabla$ representing the momentum operator in quantum physics [1] and $|\psi\rangle$ denoting the classical photon wave function analogous to quantum wave function [27], can naturally be associated with the mean wavevector as $\bar{\mathbf{k}} = \mathbf{P}/\hbar$ with the directional vector $\hat{\mathbf{k}} = \bar{\mathbf{k}}/k$ and module $k = |\bar{\mathbf{k}}|$ [27]. Here, the symbol \wedge represents the interlink between helicity and mean wavevector $\bar{\mathbf{k}}$ is local for the individual waves.

Equation (1) clearly represents that the L-spin is determined by the EM helicity solely, whereas the Eq. 2 reveals that, for an arbitrary wave with hybrid polarization, the T-spin comes from the inhomogeneities of EM wave and its transversality constraint satisfies since there is $\nabla \cdot (\nabla \times \mathbf{A}) = 0$ for an arbitrary vector \mathbf{A} . Remarkably, the L-spin is based on the interlink between the EM helicities of individual waves and their local wavevectors, rather than the mean wavevector, and thus one may possibly construct a counterintuitive L-spin that is perpendicular to mean wavevector. On the other hand, the T-spin possesses a widespread property of spin-momentum locking, which does not relate to L-spin of EM wave propagating in a homogeneous medium. In unison, the spin-momentum locking originated from the intrinsic spin-orbit coupling in Maxwell's equations is considered as a fundamental property of T-spin for an arbitrary EM field, no matter whether the propagating waves or the surface waves and guided waves.

The remarkable features of both the L-spin and T-spin in an EM field coincide the definition of intrinsic SAM in quantum physics, where photons are the spin-1 particles with SAM ($\mathbf{s} = \hbar\sigma\hat{\mathbf{k}}$, $\sigma=\pm 1$) along the direction of momentum $\mathbf{p} = \hbar\mathbf{k}\hat{\mathbf{k}}$. In a classical EM field considered here, it is widely accepted that the circularly polarized light (CPL) is corresponding to the two helical states in quantum physics [1]. Then, the

total spin of CPL is calculated as $\mathbf{S} = \hbar\sigma\hat{\mathbf{k}}$ with the directional vector of local wavevector $\hat{\mathbf{k}}$ ([Supplemental Note 1](#)). Obviously, the SAM, which is along the direction of the local wavevector, is net longitudinal ($\mathbf{S}_l = \mathbf{S}$) and depends on the EM helicity solely [\[6\]](#). This result is consistent with Eq. 2 since no inhomogeneity exists in propagating plane wave with the T-spin $\mathbf{S}_t = \nabla \times \mathbf{\Pi}/2k^2 = 0$.

Subsequently, for an elliptically polarized evanescent plane wave in an arbitrary orthogonal coordinate system (p, s, z) as shown in Fig. 1, the total SAM is $\mathbf{S} = \hbar(k^2\sigma/k_p^2)\hat{\mathbf{k}} - W\kappa/\omega k_p \hat{\mathbf{s}}$ with W, k_p and $i\kappa$ the energy density, in-plane and out-of-plane wavevectors, respectively ([Supplemental Note 2](#)). Obviously, the s -component SAM is the helix-free T-spin perpendicular to the local wavevector [\[7\]](#). However, comparing to the helicity of the propagating plane wave, the longitudinal SAM component here contains an additional factor k^2/k_p^2 , which is illogical in physics since the ‘longitudinal spins’ of photons should be constant, even in a system that the total AM is not conservative due to the breaking of inverse symmetry [\[28\]](#). On the other hand, owing to the evanescent property of wave in the z -direction, one can find that there are two types of inhomogeneities here: the intensity inhomogeneity in pz -plane normal to s -axis and the inhomogeneity of helicity density (given by the product of intensity and helicity) in the sz -plane normal to p -axis. Thus, one can expect that the T-spin has two components:

$$\mathbf{S}_t = \frac{1}{2k^2} \nabla \times \mathbf{\Pi} = -\hbar\sigma \frac{\kappa^2}{k_p^2} \hat{\mathbf{k}} - \frac{W}{\omega} \frac{\kappa}{k_p} \hat{\mathbf{s}}. \quad (3)$$

From Eq. 1, the L-spin can be calculated as $\mathbf{S}_l = \mathbf{S} - \mathbf{S}_t = \hbar\sigma\hat{\mathbf{k}}$, which coincides with that of propagating plane wave. In this way, besides the helix-free T-spin component, a hidden extraordinary T-spin that is helicity-dependent is discovered and validated theoretically. Furthermore, Eq. 3 indicates the spin-momentum locking property of evanescent plane wave, which reveals that there are four spin-momentum locked states for a generic EM field. This is consistent with the photonic spin Chern number of EM wave and indicates the photons possess \mathbb{Z}_4 topological invariance. Noteworthily, in the case that the dual symmetry between the electric and magnetic features is broken [\[17,26\]](#) and there is only a single polarized state survive, the four spin-momentum locked states would be degraded into the two helicity-independent states, which coincides with the spin-momentum locking caused by helix-free T-spin.

The aforementioned extraordinary property of EM spin can be generalized to a generic EM wave by expanding it into the superpositions of plane wave basis from the principle of the superposition of states [\[1\]](#). Here, for the sake of simplicity, we only introduce the two-waves interference since the multi-waves interference takes the same rules. The calculated results of all three types of two-waves interference, including the propagating and evanescent waves, reveal a unified relation between longitudinal and transverse spin are

$$\mathbf{S}_l = \hbar\sigma \wedge \hat{\mathbf{k}} = \hbar\sigma_1 \hat{\mathbf{k}}_1 + \hbar\sigma_2 \hat{\mathbf{k}}_2 + \hbar\sigma_{\text{inter}} \hat{\mathbf{k}}_{\text{inter}} \quad \text{and} \quad \mathbf{S}_t = \mathbf{S} - \mathbf{S}_l = \frac{1}{2k^2} \nabla \times \mathbf{\Pi}, \quad (4)$$

where the L-spin of the individual wave is $\mathbf{S}_{l1,2} = \hbar\sigma_{1,2} \hat{\mathbf{k}}_{1,2}$ along the corresponding local wavevector, respectively. The additional interferential helicity term σ_{inter} represents the ratio of the crossed polarization ellipticities between the two waves to the interferential energy, and $\hat{\mathbf{k}}_{\text{inter}}$ represents the local propagating wavevector of this interferential energy by comparing the energy density and the mean wavevector of the total interferential fields. Particularly, the integral form of Eq. 4 is $\langle \mathbf{S} \rangle = \langle \hbar\sigma_1 \hat{\mathbf{k}}_1 \rangle + \langle \hbar\sigma_2 \hat{\mathbf{k}}_2 \rangle + \langle \mathbf{S}_t \rangle$, which indicates the integral of the interferential helicity vanishes. Thus, the interferential effect is local and does not affect the conservation of AMs ([Supplemental Notes 3 and 4](#)). Noteworthily, in a rotating symmetric system such as the propagating wave in free space, the total AM is conservative and the integral T-spin is

zero. Whereas for an inverse symmetry broken system such as the evanescent wave at an interface, only z -component total AM is conservative, and hence the T-spin can carry net SAM and the integral T-spin is nonvanishing. As the dual symmetry is broken [17,26] further, there is only a single polarized state survive and the integral T-spin is zero in accord with that of the helix-free T-spin.

Obviously, even in a general framework, the T-spin originated from the inhomogeneity of field is validated. Since there must be inhomogeneity of helical density in the direction of mean wavevector for the individual wave carrying EM helicity in two-waves interference, the extraordinary helicity-dependent T-spin will present universally. Besides the extraordinary T-spin, we discover an extraordinary L-spin (Figs. 2d, 2e, 2k, 2l) perpendicular to the mean wavevector which does not possess the property of spin-momentum locking. As the polarization ellipticities of the individual wave are opposite exactly, it can be obtained that the interferential helicity term σ_{inter} vanishes and the total helicity is along the mean wavevector of the two-waves interferences both in free space (Fig. 2a) and at optical interface (Fig. 2h). However, from Eq. 4, there will be a superposition state of T-spin exist definitely for the propagating wave (Figs. 2d-e) and surface wave (Figs. 2k-l). As the propagating directions of these two waves are inverted (Figs. 2b-c and Figs. 2i-j), the corresponding L-spins remain unchanged, while the directions of T-spins are inverted simultaneously owing to the property of spin-momentum locking. Noteworthily, for the propagating wave in free space, the integral T-spins (Figs. 2f-g) vanish due to the rotating symmetry, whereas the integral T-spins of surface waves (Figs. 2m-n) are non-zero due to the breaking of inverse symmetry. The aforementioned theoretical results reveal that the extraordinary L-spin and T-spin are widely existed in the generic EM field.

Finally and most importantly, from Eq. 3, it can be found that the extraordinary T-spin is antiparallel to the mean wavevector. Actually, this is a general property of extraordinary T-spin and widely exist in a generic EM field. Previously, the generation of this inverted helical component was explained based on the evolution of geometric phase in EM systems [6,14]. Here, this inverted helical component can be classified to ‘longitudinal’ part of T-spin which demonstrate the extraordinary T-spin is closely related to the geometric phase of EM systems (see [Supplemental Note 6](#) for an example of focused circular polarizations).

To validate the extraordinary properties of EM spins, we build the scanning imaging systems to mapping the three components of SAMs for the focused circularly polarized lights separately (see [Supplemental Notes 7 and 8](#) for details). The experimental results in Fig. 3 reveal that the two transverse components of SAM in the focused field remain unchanged as the incident light alters from right-handed circular polarization (RCP) to left-handed circular polarization (LCP), which is corresponding to the helicity-independent T-spin. On the contrary, the z component SAM, which contains the L-spin and extraordinary T-spin, is helicity-dependent. If not, the absolute values of two S_z distributions as shown in Figs. 3f and 3l would be discrepant. The experimental results match well with theoretical analyses, which demonstrate the extraordinary T-spin and spin-momentum locking properties of EM spins.

To summarize, we uncover and demonstrate, both theoretically and experimentally, the underlying physical difference between the T-spin and L-spin. First, the L-spin is determined by the EM helicity, while the T-spin is originated from the inhomogeneities of EM field. Second, even in a generic EM wave field carrying helicities, the T-spin is locked with the momentum of EM field, while the L-spin in a homogeneous medium does not possess the property of spin-momentum locking. We emphasize here that the spin-momentum locking of T-spin is originated from the intrinsic SOI feature of the Maxwell’s theory in real space, which is different from the spin-momentum locking by engineering the extrinsic SOI in topological photonics [29]. However, the resulted phenomena of these two physical processes are analogous. There does not exist an

EM state whose T-spin vector can be positive and negative concurrently as it propagates in a direction. Akin to topological photonics, one can also design artificial photonic structures sustaining the desired structured light and spin states to achieve the on-chip applications [30]. Third, from the rigorous argument, we discover an extraordinary T-spin that is local helicity-dependent, which leads to that the accompanying spin-momentum locking is also helicity-dependent. Particularly, in rotational symmetric system, the integral full T-spin vector should be helicity-independent, which is consistent with the principle of conservation of total AM physically. This explains why there is only T-spin exist in the focusing field of an incident wave with orbital AM. Whereas in a system with broken inverse symmetry, the integral T-spin can be non-zero. Fourth, the extraordinary T-spin determines the inverted helical component that is arisen from evolution of the geometric phases of EM systems. Noteworthily, the properties of helicity, spin-momentum locking and geometric phase related T-spins in a generic EM field are different from those of the T-spins of a single polarized mode dramatically. The primary properties of these two spins and their distinction are exhibited in **Table 1**. Moreover, whether the L-spin or the T-spin, they can be arranged in three-dimensional, and thus the structured property of T-spin can be flexibility designed to obtain various photonic chiral spin textures. The findings deepen our understanding of EM spin and explore the novel applications in manipulation, imaging, communication, nanometrology and on-chip optoelectronic devices.

Acknowledgements

This work was supported, in part, by Guangdong Major Project of Basic Research No. 2020B0301030009, National Natural Science Foundation of China grants U1701661, 61935013, 62075139, 61427819, 61622504, and 61705135, leadership of Guangdong province program grant 00201505, Science and Technology Innovation Commission of Shenzhen grants JCYJ20200109114018750, Shenzhen Peacock Plan KQTD20170330110444030. L.D. acknowledges the support given by the Guangdong Special Support Program.

Author contributions

All authors contributed to the article.

Competing interests

The authors declare no competing interests.

Data availability

The data that support the plots within this paper and other findings of this study are available from the corresponding author upon reasonable request.

References:

1. J. J. Sakurai, *Modern quantum mechanics*, Addison-Wesley, San Francisco, CA, 1994.
2. J. D. Jackson, *Classical Electrodynamics*, third ed., New Jersey, Wiley, 1999.
3. Y. Long, J. Ren, and H. Chen, Intrinsic spin of elastic waves, *Proc. Natl. Acad. Sci. USA* 115(40), 9951-9955 (2018).
4. K. Y. Bliokh and F. Nori, Spin and orbital angular momenta of acoustic beams, *Phys. Rev. B* 99, 174310:1-9 (2019).
5. M. S. Longuet-Higgins, Spin and angular momentum in gravity waves, *Journal of Fluid Mechanics*, 97(1), 1-25 (1980).
6. K. Y. Bliokh, F. J. Rodríguez-Fortuño, F. Nori, and A. V. Zayats, Spin-orbit interactions of light, *Nat. Photonics* 9(12), 796-808 (2015).
7. A. Aiello, P. Banzer, M. Neugebauer, and G. Leuchs, From transverse angular momentum to photonic wheels, *Nat. Photon.* 9(12), 789-795 (2015).

8. K. Y. Bliokh and F. Nori, Transverse and longitudinal angular momenta of light, *Phys. Rep.* 592, 1–38 (2015).
9. A.Y. Bekshaev, K. Y. Bliokh, and F. Nori, Transverse spin and momentum in two-wave interference, *Phys. Rev. X* 5, 011039:1–9 (2015).
10. J. S. Eismann, L. H. Nicholls, D. J. Roth, M. A. Alonso, P. Banzer, F. J. Rodríguez-Fortuño, A. V. Zayats, F. Nori, and K. Y. Bliokh, Transverse spinning of unpolarized light, *Nat. Photonics* 15, 156–161 (2020).
11. L. P. Du, A. P. Yang, A. V. Zayats, and X. C. Yuan, Deep-subwavelength features of photonic skyrmions in a confined electromagnetic field with orbital angular momentum, *Nat. Phys.* 15, 650–654 (2019).
12. Y. Dai, Z. Zhou, A. Ghosh, R. S. K. Mong, A. Kubo, C.-B. Huang, and H. Petek, Plasmonic topological quasiparticle on the nanometre and femtosecond scales, *Nature* 588, 616–619 (2020).
13. L. Allen, M. W. Beijersbergen, R. J. Spreeuw, and J. P. Woerdman, Orbital angular momentum of light and the transformation of Laguerre-Gaussian laser modes, *Phys. Rev. A* 45(11), 8185–8189 (1992).
14. P. Shi, A. Yang, F. Meng, J. Chen, Y. Zhang, Z. Xie, L. Du, and X.-C. Yuan, Optical near-field measurement for spin-orbit interaction of light, *Progress in Quantum Electronics* 79, 100341:1–20 (2021).
15. F. J. Rodríguez-Fortuño, G. Marino, P. Ginzburg, D. O'Connor, A. Martínez, G. A. Wurtz, A. V. Zayats, Near-field interference for the unidirectional excitation of electromagnetic guided modes, *Science* 340, 328–330 (2013).
16. J. Petersen, J. Volz, and A. Rauschenbeutel, Chiral nanophotonic waveguide interface based on spin-orbit interaction of light, *Science* 346(6205), 67–71 (2014).
17. K. Y. Bliokh, D. Smirnova, and F. Nori, Quantum spin Hall effect of light, *Science* 348, 1448–1451 (2015).
18. M. Antognazzi, C. R. Bermingham, R. L. Harniman, S. Simpson, J. Senior, R. Hayward, H. Hoerber, M. R. Dennis, A. Y. Bekshaev, K. Y. Bliokh and F. Nori, Direct measurements of the extraordinary optical momentum and transverse spin-dependent force using a nano-cantilever, *Nat. Phys.* 12, 731–735 (2016).
19. G. Araneda, S. Walser, Y. Colombe, D. B. Higginbottom, J. Volz, R. Blatt, and A. Rauschenbeutel, Wavelength-scale errors in optical localization due to spin-orbit coupling of light, *Nature Physics* 15, 17–21 (2019).
20. Z. Shao, J. Zhu, Y. Chen, Y. Zhang, and S. Yu, Spin-orbit interaction of light induced by transverse spin angular momentum engineering, *Nat. Commun.* 9, 926:1–11 (2018).
21. M. Neugebauer, P. Wozniak, A. Bag, G. Leuchs, and Peter Banzer, Polarization-controlled directional scattering for nano-scopic position sensing, *Nat. Commun.* 7, 11286:1–6 (2016).
22. P. Lodahl, S. Mahmoodian, S. Stobbe, A. Rauschenbeutel, P. Schneeweiss, J. Volz, H. Pichler, and P. Zoller, Chiral quantum optics, *Nature* 541, 473–480 (2017).
23. A. Forbes, Michael de Oliveira, and Mark R. Dennis, Structured light, *Nature Photonics* 15, 253–262 (2021).
24. A. Aiello and P. Banzer, The ubiquitous photonic wheel, *J. Opt.* 18, 085605:1–8 (2016).
25. N. Nagaosa and Y. Tokura, Topological properties and dynamics of magnetic skyrmions, *Nat. Nanotechnology* 8, 899–911 (2013).
26. P. Shi, L.-P. Du, C.-C. Li, A. Zayats, and X.-C. Yuan, Transverse spin dynamics in structured electromagnetic guided waves, *PNAS* 118(6), e2018816118:1–6 (2021).
27. M. V. Berry, Optical currents, *J. Opt. Pure Appl. Opt.* 11(9), 094001:1–12 (2009).
28. R. P. Cameron and S. M. Barnett, Electric-magnetic symmetry and Noether's theorem, *New J. Phys.* 14, 123019:1–27 (2012).
29. L. Lu, John D. Joannopoulos, and M. Soljačić, Topological photonics, *Nature Photonics* 8, 821–829 (2014).
30. L. Peng, L. Duan, K. Wang, F. Gao, L. Zhang, G. Wang, Y. Yang, H. Chen, and S. Zhang, Transverse photon spin of bulk electromagnetic waves in bianisotropic media, *Nat. Photon.* 13, 878–882 (2019).

Figures and Figure captions:

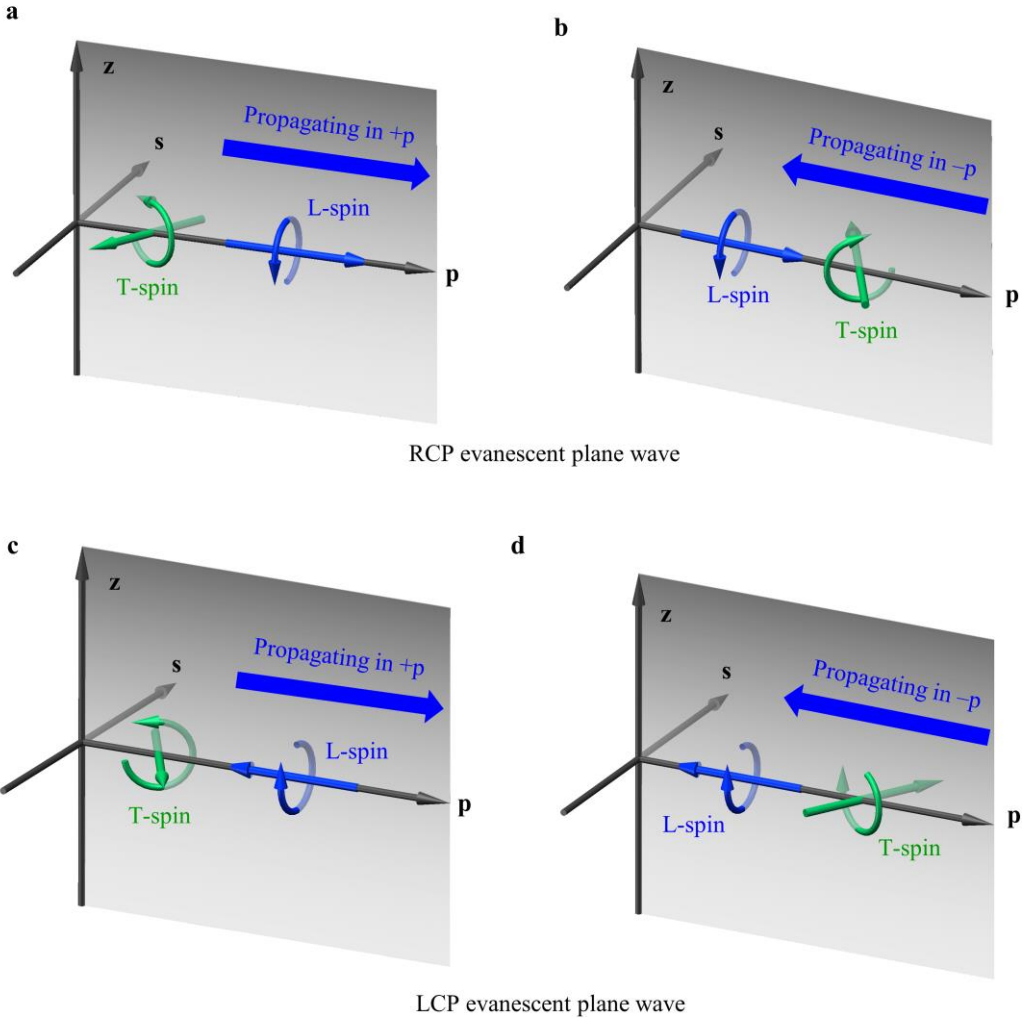


Figure 1 | Spin-momentum locking properties of extraordinary transverse optical spins. **a-b**, The L-spin and T-spin of right-handed circularly polarized (RCP) evanescent plane wave propagating in the **a**, $+p$ -direction and **b**, $-p$ -direction; **c-d**, the L-spin and T-spin of left-handed circularly polarized (LCP) evanescent plane wave propagating in the **c**, $+p$ -direction and **d**, $-p$ -direction. For the evanescent plane wave decaying exponentially in the z -direction, there are two types of inhomogeneities: the inhomogeneities of helicity density in the sz -plane normal to p -axis and the inhomogeneity of intensity in the zp -plane normal to s -axis. Thus, the T-spins have two components (s and p components). The p component T-spin originated from the inhomogeneity of helicity density is helicity-dependent and inverted to the direction of longitudinal spin. Therefore, the direction vector of T-spin for the circularly polarized evanescent plane wave is deflected compared to that of the single-polarized field. Nevertheless, the nature of spin-momentum locking is generally satisfied. The exhibited four spin-momentum locking states are consistent with the photonic spin Chern number, which demonstrates that the photons satisfy the Z4 topological invariance.

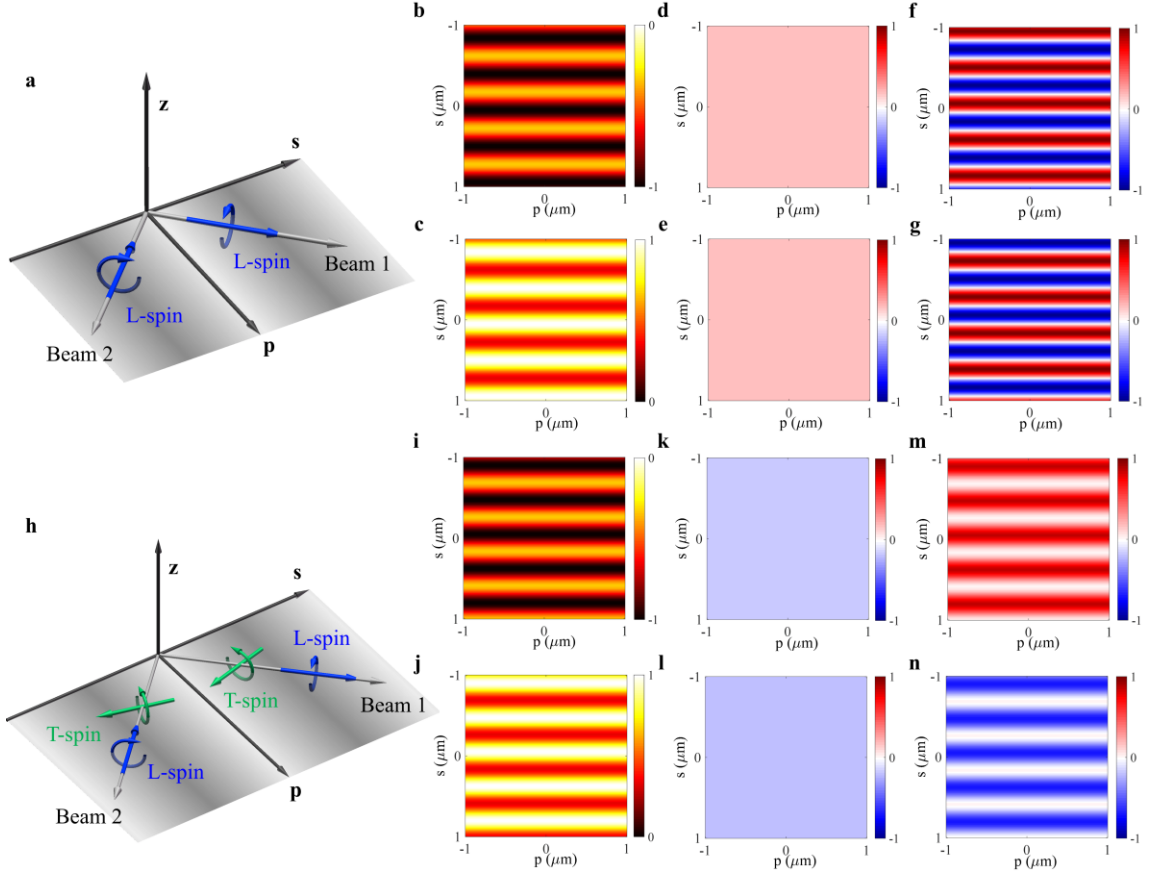


Figure 2 | Extraordinary L-spin and T-spin in two-waves interference. **a**, Schematic diagram of interference in ps -plane between two plane waves carrying opposite helicities. **b**, **c**, the spatial distribution of canonical momentum (only contains p -component) and the corresponding **d**, **e**, s -component L-spins and **f**, **g**, z -component helicity-independent T-spins. The canonical momentum determines the mean wavevector and the propagating direction. Here, the whole s -component SAM is the extraordinary L-spin, which is perpendicular to the mean wavevector. The whole z -component SAM is corresponding to the helix-free T-spin. As the canonical momentum is inverted, the s -component L-spin remain unchanged while the z -component T-spins reverse. **h**, Schematic diagram of interference in ps -plane between two evanescent plane waves carrying opposite helicities. **i**, **j**, the spatial distribution of canonical momentum (only contains p -component) and the corresponding **k**, **l**, s -component L-spins and **m**, **n**, s -component helicity-dependent T-spins. Here, we do not exhibit the distributions of the helicity-independent T-spins in the z -direction since the distributions are similar to **f** and **g**. The canonical momentum determines the mean wavevector and the propagating direction. Part of the uniform s -component SAM is the extraordinary L-spin, which is perpendicular to the mean wavevector, whereas part of the nonuniform s -component SAM is the extraordinary helicity-dependent T-spin. As the canonical momentum is inverted, the s -component L-spin remain unchanged while the s -component T-spins reverse. Noteworthily, the integral T-spin is nonzero stemming from the breaking of rotating symmetry. The amplitudes of two wave are $A_{s1}=1$, $A_{p1}=5+2i$, and $A_{s2}=1$, $A_{p2}=5-2i$. The wavelength is 632.8nm.

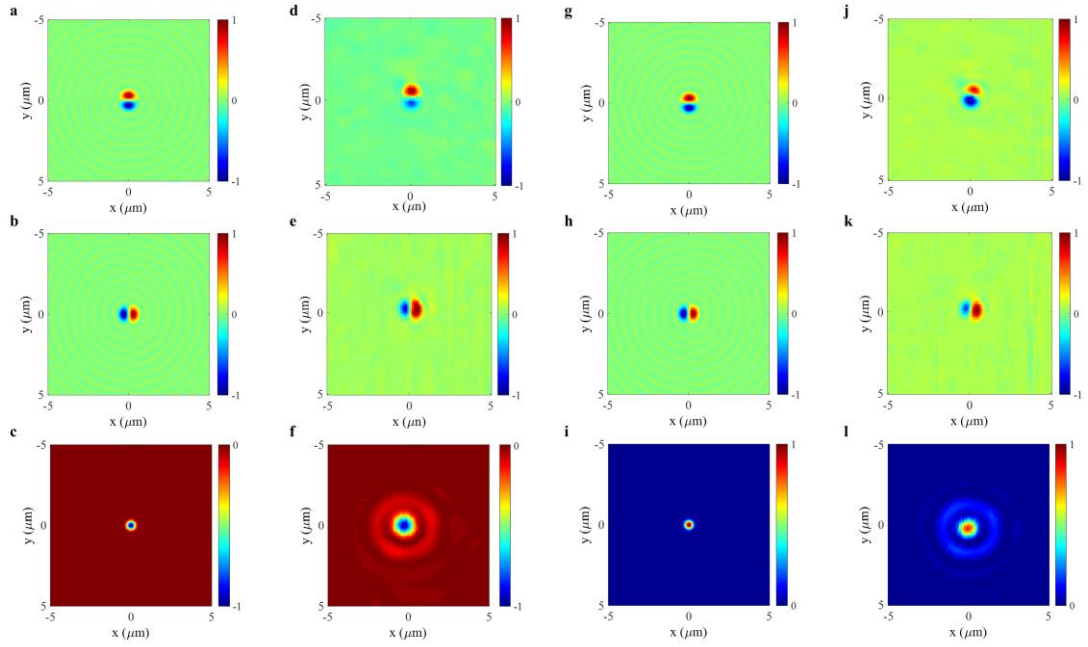


Figure 3 | Experimental validation of the spin-momentum locking and T-spin. **a-f**, The theoretical **a**, S_x , **b**, S_y and **c**, S_z and the corresponding experimental **d**, S_x , **e**, S_y and **f**, S_z of the focused LCP light; **j-l**, the theoretical **g**, S_x , **h**, S_y and **i**, S_z and the corresponding experimental **j**, S_x , **k**, S_y and **l**, S_z of the focused RCP light. Here, we use the traditional Cartesian coordinates (x , y , z) instead of orthogonal coordinates (p , s , z). The optical axis is along the z -direction. The experimental SAM distributions match well with those of theoretical results. The details of theoretical calculations can be found in [Supplemental Note 6](#). The experimental results and the corresponding error analysis can be found in [Supplemental Notes 7 and 8](#). As the incident wave is changed from the LCP light to RCP light, the x and y components of SAMs, which can be regarded as the helicity-independent T-spin, remain unchanged. On the contrary, the sign of z component of SAM alters from positive to negative as the helicity of incident light changes. The z component of SAM contains two contributions: the L-spin and the longitudinal component of T-spin. Thus, the longitudinal component of T-spin is helicity-dependent. If not, the distributions would be altered for **f** and **l**. The wavelength is fixed at 632.8nm in the experiments. The scanned region is $10\mu\text{m} \times 10\mu\text{m}$ and the grid size is 100nm. The (**d**, **e**, **j**, **k**) is normalized to the maximum and the numerical aperture of this focusing system is 0.5; and the (**f**, **l**) is normalized to their maximum and the numerical aperture of this focusing system measured the S_z is 0.7.

Table 1 | Underlying physical difference of T-spin and L-spins for a generic EM field

Properties	EM T-spin	EM L-spin
Physical origin	Inhomogeneities/structure properties of EM field	EM helicity σ
Direction of spin vector	Antiparallel and perpendicular to local wave vector $\hat{\mathbf{k}}$.	Parallel to local wave vector $\hat{\mathbf{k}}$.
Deterministic equation	$\mathbf{S}_t = \mathbf{S} - \mathbf{S}_l = \frac{1}{2k^2} \nabla \times \mathbf{H}$	$\mathbf{S}_l = \hbar \sigma \wedge \hat{\mathbf{k}}$
Is locked with momentum?	Yes.	No.
Is local helicity-dependent?	Local helicity-dependent if there is inhomogeneity of helicity density.	Yes.
Is integral helicity-dependent?	Integral helicity-dependent if the rotating symmetry is broken.	Yes.
Is geometric phase dependent?	Helicity-dependent T-spin determine the geometric phase.	Yes.